

A distributive mechanism for twophoton meanfrequency absorption

David L. Andrews and Kevin P. Hopkins

Citation: [The Journal of Chemical Physics](#) **89**, 4461 (1988); doi: 10.1063/1.454785

View online: <http://dx.doi.org/10.1063/1.454785>

View Table of Contents: <http://scitation.aip.org/content/aip/journal/jcp/89/8?ver=pdfcov>

Published by the [AIP Publishing](#)

Articles you may be interested in

[Two-photon absorption in solution by means of time-dependent density-functional theory and the polarizable continuum model](#)

J. Chem. Phys. **122**, 244104 (2005); 10.1063/1.1944727

[Vibration and two-photon absorption](#)

J. Chem. Phys. **116**, 9729 (2002); 10.1063/1.1477179

[Cooperative meanfrequency absorption: A twobeam twophoton process](#)

J. Chem. Phys. **86**, 2453 (1987); 10.1063/1.452098

[Cooperative twophoton absorption](#)

J. Chem. Phys. **78**, 1088 (1983); 10.1063/1.444891

[TWOPHOTON ABSORPTION IN ZnS](#)

Appl. Phys. Lett. **10**, 265 (1967); 10.1063/1.1754803



A distributive mechanism for two-photon mean-frequency absorption

David L. Andrews and Kevin P. Hopkins

School of Chemical Sciences, University of East Anglia, Norwich NR4 7TJ, England

(Received 18 January 1988; accepted 28 June 1988)

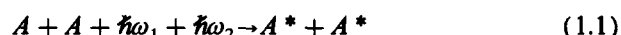
This paper describes a new mechanism for the concerted mean-frequency absorption process $A + A + \hbar\omega_1 + \hbar\omega_2 \rightarrow A^* + A^*$. In contrast to a mechanism described previously, this effect can be subject to the normal selection rules for single-photon absorption, and is mediated by virtual photon coupling. Rate equations are given for molecules in a fluid, van der Waals molecules, and chromophore pairs in polyatomic molecules. The dependence of the absorption rate on the separation of the interacting pair is then examined in detail. An analogy is drawn between the long-range limit of the absorption rate and a process of hyper-Raman scattering followed by single-photon absorption. It is demonstrated that the two processes are equivalent where the molecular separation is large enough that the virtual photon can be considered as real and physically identifiable.

I. INTRODUCTION

Cooperative optical transitions are observed in a wide variety of media. Such processes occur in the gas phase as a result of atomic collisions¹; at the other extreme, they are observed in the solid state as a result of interaction between impurity centers and host atoms.² Such processes also play a role in chemical reactions observed in high-pressure gases³ and in matrix isolation.⁴ The diversity in mechanism between these effects is enormous, but a common factor is a substantial contribution from pairs of molecules or other entities which are in close proximity. This is the final paper of a series⁵⁻⁷ in which the methods of molecular quantum electrodynamics (QED) are applied to concerted *two-photon* absorption. Here, two chemical centers undergo concerted excitation involving the absorption of two photons from intense laser beams. The two centers which may, or may not, be chemically equivalent can be either distinct chromophores in a single molecule, or completely separate molecules. Where the two centers are chemically identical, the recently coined term *bicimer*⁸ appropriately describes the result of the excitation.

Two particular classes of proximity-induced two-photon absorption (in the past generally referred to as a cooperative process) are of special interest. These are where there is (a) single-frequency excitation of a chemically inequivalent pair, or (b) two-frequency excitation of a chemically equivalent pair, Fig. 1. Each class may be further divided into two cases of interest: (i) where one real photon is absorbed at each of the two centers, and (ii) where both real photons are absorbed at a single center. To clarify this distinction, the former (i) is henceforth referred to as the *cooperative* mechanism, and the latter (ii) the *distributive* mechanism. Thus proximity-induced two-photon absorption leads to four distinct cases of interest, as represented by the time-ordered diagrams of Fig. 2. Three of these have been dealt with in previous papers,⁵⁻⁷ and attention is now drawn to the fourth case, that of two-frequency excitation of a chemically equivalent pair, where two photons are absorbed at one center, and its partner is excited solely by a virtual photon interaction.

The two chemical centers have identical composition and are excited through a distributive two-photon absorption process at the common focus of two laser beams of frequencies ω_1 and ω_2 , which may or may not be collinear. This process is represented by the energy level diagram of Fig. 1(b) and the equation



in which the asterisk denotes an excited state of A . The two frequencies ω_1 and ω_2 are deliberately chosen to be a region

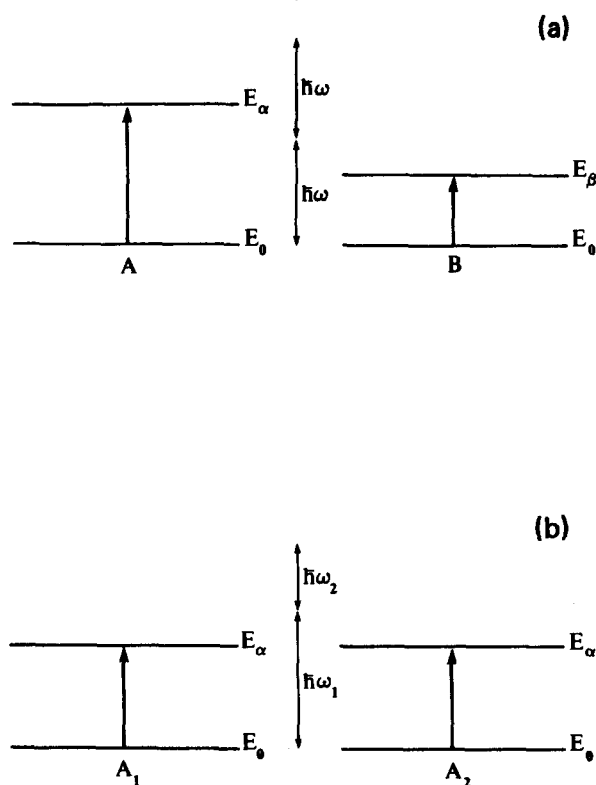


FIG. 1. Energy level diagrams for two particular cases of proximity-induced two-photon absorption; (a) with single-frequency excitation of a chemically inequivalent pair, and (b) with two-frequency excitation of a chemically equivalent pair.

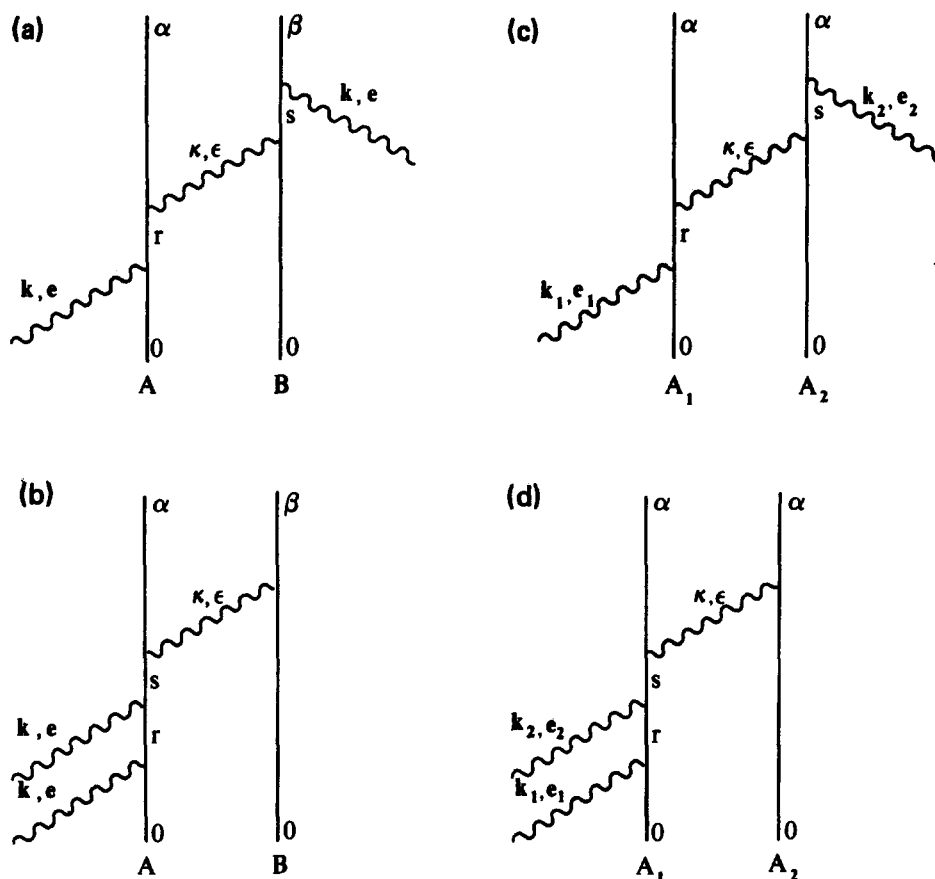


FIG. 2. Typical time-ordered diagrams representing four distinct cases of concerted two-photon absorption: (a) the single-frequency cooperative mechanism, (b) the single-frequency distributive mechanism, (c) the two-frequency cooperative mechanism, and (d) the two-frequency distributive mechanism.

where single-photon absorption cannot lead to the excitation of either center (i.e., A has no absorption bands in the frequency region of either ω_1 or ω_2). For the case under consideration we also specify that the selection rules permit excitation of the final state, A^* , through a one-photon electric-dipole interaction, but not through a two-photon interaction. The energetics of the process can thus be described by

$$\frac{1}{2}(\hbar\omega_1 + \hbar\omega_2) = E_{\alpha 0} \quad (1.2)$$

and

$$\hbar\omega_1, \hbar\omega_2 \neq E_{\alpha 0}, \quad (1.3)$$

clearly illustrating the mean-frequency absorption nature of the process.

II. GENERAL RESULTS

Analysis of the distributive mechanism for mean-frequency two-photon absorption needs to be based upon QED methods,^{9,10} and the detailed theory for the calculations has been presented in earlier work.⁷ The transition matrix element for the process is constructed with the aid of 48 time-ordered diagrams, four of which are illustrated in Fig. 3. The only diagrams to contribute are those in which both laser photons are absorbed at one center, leading to excitation of the other participating center by a virtual photon interac-

tion. For the distributive mechanism under consideration, the possibility of each real photon being absorbed at a different center is excluded as this would necessitate a forbidden two-photon excitation process at each center. The total matrix element for the process can be expressed as follows:

$$M_{fi} = (-\hbar c/2V\epsilon_0)(n_1 n_2 k_1 k_2)^{1/2} e_{1i} e_{2j} \times \{ \chi_{ijk}^{\alpha 0}(A_1) \mu_i^{\alpha 0}(A_2) V_{kl}(\gamma, \mathbf{R}) + \chi_{ijk}^{\alpha 0}(A_2) \mu_i^{\alpha 0}(A_1) \bar{V}_{kl}(\gamma, \mathbf{R}) e^{i\mathbf{u} \cdot \mathbf{R}} \}, \quad (2.1)$$

where the implied summation convention has been incorporated for repeated tensor indices. Here n_1, n_2 are the number of photons of wave vector $\mathbf{k}_1, \mathbf{k}_2$ and polarization vector $\mathbf{e}_1, \mathbf{e}_2$, respectively, in the quantization volume V ; \mathbf{u} represents the wave vector sum $(\mathbf{k}_1 + \mathbf{k}_2)$ and \mathbf{R} denotes the vector displacement $\mathbf{R}(A_2) - \mathbf{R}(A_1)$. The parameter γ is defined by $\hbar\gamma = E_{\alpha 0}$ and represents the conservation energy effectively transferred between the two centers by the virtual photon. The complex retarded resonance electric dipole-electric dipole interaction $V_{kl}(\gamma, \mathbf{R})$ is given by^{11,12};

$$V_{kl}(\gamma, \mathbf{R}) = (1/4\pi\epsilon_0 R^3) [(\delta_{kl} - 3\hat{\mathbf{R}}_k \hat{\mathbf{R}}_l) (e^{i\gamma R} - i\gamma R e^{i\gamma R}) - (\delta_{kl} - \hat{\mathbf{R}}_k \hat{\mathbf{R}}_l) \gamma^2 R^2 e^{i\gamma R}], \quad (2.2)$$

and arises when a summation over virtual photon wave vec-

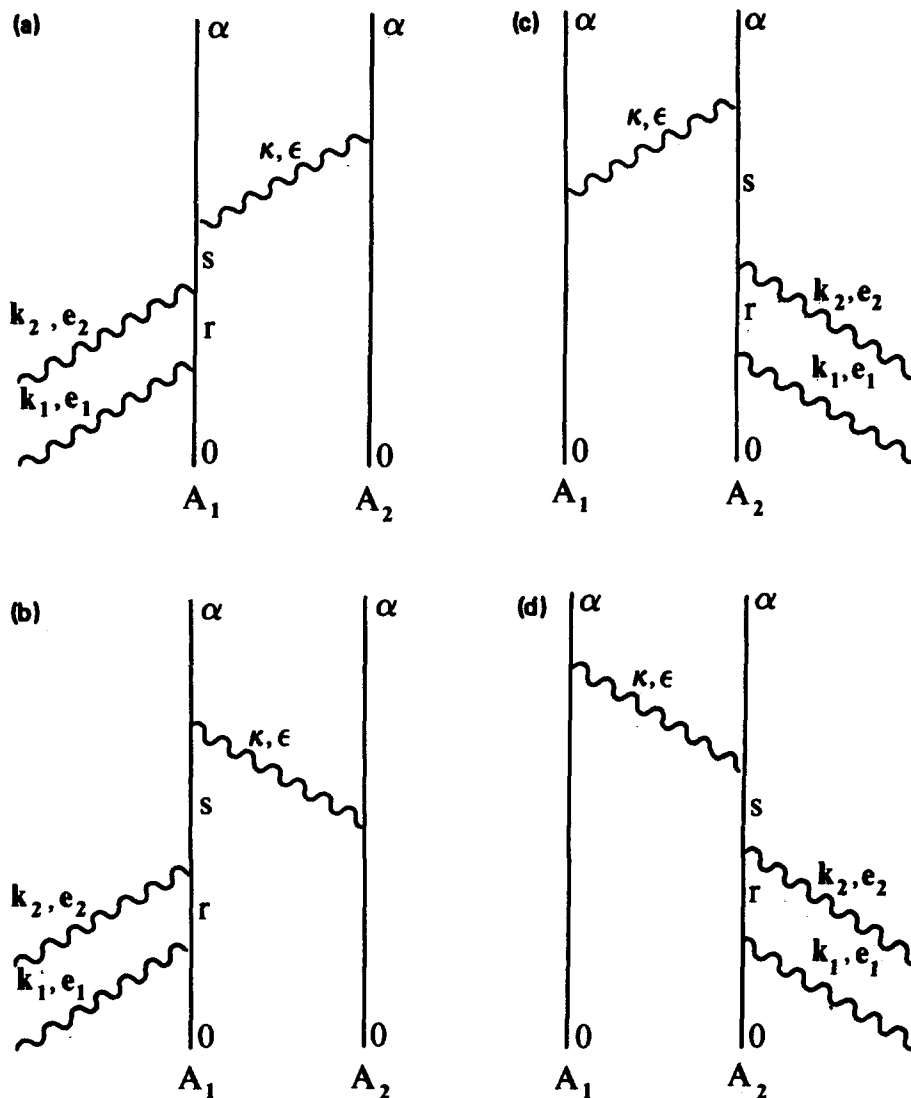


FIG. 3. Four typical time-ordered diagrams for distributive two-frequency two-photon absorption.

tors and polarizations is performed. The molecular tensor $\chi_{ijk}^{\alpha\alpha}$ is a more general form of three tensors which have featured in previous work on multiphoton processes; one is the $\chi_{ijk}^{\alpha\alpha}$ tensor arising in single-frequency distributive two-photon

absorption,⁶ and another is the T_{ijk} tensor which appears in the theory of three-photon absorption.¹³ It is also exactly identical to the two-frequency hyper-Raman transition tensor $\beta_{ijk}^{\alpha\alpha}$,¹⁴ and can be expressed as:

$$\chi_{ijk}^{\alpha\alpha}(A_1) = \sum_{s,r} \left[\frac{\mu_i^{\alpha\alpha}(A_1)\mu_j^{sr}(A_1)\mu_k^{\alpha\alpha}(A_1)}{(E_{0s} + \hbar ck_1 + \hbar ck_2)(E_{0r} + \hbar ck_1)} + \frac{\mu_i^{\alpha\alpha}(A_1)\mu_j^{\alpha\alpha}(A_1)\mu_k^{sr}(A_1)}{(E_{\alpha s} - \hbar ck_2)(E_{0r} + \hbar ck_1)} \right. \\ \left. + \frac{\mu_i^{sr}(A_1)\mu_j^{\alpha\alpha}(A_1)\mu_k^{\alpha\alpha}(A_1)}{(E_{\alpha r} - \hbar ck_1 - \hbar ck_2)(E_{\alpha s} - \hbar ck_2)} + \frac{\mu_i^{sr}(A_1)\mu_j^{\alpha\alpha}(A_1)\mu_k^{\alpha\alpha}(A_1)}{(E_{0s} + \hbar ck_1 + \hbar ck_2)(E_{0r} + \hbar ck_2)} \right. \\ \left. + \frac{\mu_i^{\alpha\alpha}(A_1)\mu_j^{\alpha\alpha}(A_1)\mu_k^{sr}(A_1)}{(E_{0r} + \hbar ck_2)(E_{\alpha s} - \hbar ck_1)} + \frac{\mu_i^{\alpha\alpha}(A_1)\mu_j^{sr}(A_1)\mu_k^{\alpha\alpha}(A_1)}{(E_{\alpha r} - \hbar ck_1 - \hbar ck_2)(E_{\alpha s} - \hbar ck_1)} \right]. \quad (2.3)$$

Applying the Fermi golden rule to Eq. (2.1) yields the rate equation

$$\Gamma = K e_{i_1} e_{j_2} \bar{e}_{1m} \bar{e}_{2n} [\chi_{ijk}^{\alpha\alpha}(A_1)\mu_i^{\alpha\alpha}(A_2)\chi_{mno}^{\alpha\alpha}(A_1)\bar{\mu}_p^{\alpha\alpha}(A_2)V_{kl}(\gamma, \mathbf{R})\bar{V}_{op}(\gamma, \mathbf{R}) \\ + \chi_{ijk}^{\alpha\alpha}(A_2)\mu_i^{\alpha\alpha}(A_1)\chi_{mno}^{\alpha\alpha}(A_2)\bar{\mu}_p^{\alpha\alpha}(A_1)V_{kl}(\gamma, \mathbf{R})\bar{V}_{op}(\gamma, \mathbf{R}) \\ + \chi_{ijk}^{\alpha\alpha}(A_1)\mu_i^{\alpha\alpha}(A_2)\chi_{mno}^{\alpha\alpha}(A_2)\bar{\mu}_p^{\alpha\alpha}(A_1)V_{kl}(\gamma, \mathbf{R})\bar{V}_{op}(\gamma, \mathbf{R})e^{i\mathbf{h}\cdot\mathbf{R}} \\ + \chi_{ijk}^{\alpha\alpha}(A_2)\mu_i^{\alpha\alpha}(A_1)\chi_{mno}^{\alpha\alpha}(A_1)\bar{\mu}_p^{\alpha\alpha}(A_2)V_{kl}(\gamma, \mathbf{R})\bar{V}_{op}(\gamma, \mathbf{R})e^{-i\mathbf{h}\cdot\mathbf{R}}], \quad (2.4)$$

where

$$K = \frac{\pi \rho_f I_1 I_2}{2 \hbar c^2 \epsilon_0^4}, \quad (2.5)$$

and where I_1 and I_2 represent the irradiances of the two incident beams

The general result for the rate, Eq. (2.4), is directly applicable to any system where the two molecules or chromophores involved in the absorption process are held in a fixed orientation both with respect to the laser beams and with respect to one another. This case would arise, for example, in a molecular crystal. To derive a rate equation applicable to fluid media it is necessary to perform averaging procedures which have been discussed in detail previously.⁷ Initially, a rotational average of Eq. (2.4) is performed to account for the random orientation of the A_1 - A_2 system. This requires both phased¹⁵ and unphased¹⁶ fourth-rank tensor averages, and the result is most concisely expressed in matrix form cast in terms of polarization parameters $A^{(j;p)}$ and molecular tensor invariants $T^{(j;q)}(\xi_1, \xi_2, \xi_3, \xi_4)$ given by

$$A^{(j;p)} = e_{1i} e_{2j} \bar{e}_{1k} \bar{e}_{2l} U_{ijkl}^{(4;j;p)}(\hat{\mathbf{u}}), \quad (2.6)$$

$$T^{(j;q)}(\xi_1, \xi_2, \xi_3, \xi_4) = \chi_{\lambda\mu\pi}^{\alpha 0}(\xi_1) \mu_{\rho}^{\alpha 0}(\xi_2) \bar{\chi}_{\nu\sigma}^{\alpha 0}(\xi_3) \\ \times \bar{\mu}_{\tau}^{\alpha 0}(\xi_4) V_{\pi\rho}(\gamma, \mathbf{R}) \bar{V}_{\sigma\tau}(\gamma, \mathbf{R}) \\ \times W_{\lambda\mu\nu\sigma}^{(4;j;q)}(\hat{\mathbf{R}}), \quad (2.7)$$

where $U_{ijkl}^{(4;j;p)}(\hat{\mathbf{u}})$ and $W_{\lambda\mu\nu\sigma}^{(4;j;q)}(\hat{\mathbf{R}})$ are tensor projections given explicitly in Ref. 15. The explicit form of the polarization parameters is given in Ref. 7 as Table I. The molecular tensor invariants for the distributive mechanism differ from those applying to the cooperative mechanism, however, and are explicitly listed in the Appendix to this paper. The rotationally averaged rate can thus be expressed as

$$\Gamma = K \left\{ \sum_{p,q} g_{(4,0)}^{pq} A^{(0;p)} T^{(0;q)}(A_1, A_2, A_1, A_2) \right. \\ \left. + \sum_{j=0}^4 \sum_{p,q} \frac{(2j)!}{2^j(j!)^2} i^j j_j(\alpha) g_{(4,j)}^{pq} A^{(j;p)} \right. \\ \left. \times T^{(j;q)}(A_1, A_2, A_2, A_1) \right\} + \{A_1 \leftrightarrow A_2\}. \quad (2.8)$$

Here $j_j(\alpha)$ denote the spherical Bessel functions of order j , where $\alpha = |\mathbf{u}|R$ and $g_{(4,j)}^{pq}$ are numerical coefficients which may also be found tabulated in the literature.¹⁷

Equation (2.8) applies to the situation where the two absorbing sites are held in fixed position relative to one another, but where the pair is free to rotate. This is the case, for example, when A_1 and A_2 represent two chromophores in a single, relatively large molecule, or else a van der Waals dimer. The fully averaged result applicable to the case where the two centers are additionally free to rotate with respect to one another may be represented by an equation equivalent to Eq. (2.8) with every $T^{(j;q)}(\xi_1, \xi_2, \xi_3, \xi_4)$ replaced by its rotational average $\langle\langle T^{(j;q)}(\xi_1, \xi_2, \xi_3, \xi_4) \rangle\rangle$.

The 19 different polarization parameters, represented by $A^{(j;p)}$, allow a substantial degree of experimental flexibility. As this set of parameters is identical to the set arising in the case of cooperative two-beam two-photon absorption, it is not appropriate to elaborate further on the polarization dependence. However, it is noted that the $T^{(j;q)}(\gamma_1, \gamma_2)$ con-

tained in Ref. 7 need to be replaced by $T^{(j;q)}(\xi_1, \xi_2, \xi_3, \xi_4)$ to obtain the equivalent results for the distributive case, and the quantity $(\omega_1 - \omega_2)$ appearing in Eqs. (5.1)–(5.6) should be replaced with $(\omega_1 + \omega_2)$.

III. LONG-RANGE CONTRIBUTIONS

In the formalism of quantum electrodynamics, both cooperative and distributive two-photon absorption are considered to be mediated through radiationless Coulombic intermolecular interactions, based on virtual photon coupling. Within the electric-dipole approximation, the involvement of a virtual photon in any particular mechanism leads to appearance of the complex retarded resonance interaction tensor $V_{kl}(\gamma, \mathbf{R})$ in the matrix element of the quantum electrodynamical calculations. The appropriate form for $V_{kl}(\gamma, \mathbf{R})$ in the near zone, ($\gamma R \ll 1$), has an R^{-3} dependence, leading to an R^{-6} dependence in the overall rate. However, this R^{-6} dependence is modified by retardation effects at large separations, producing an R^{-2} character in the rate equation. Thus, the long-range ($\gamma R \gg 1$) result can be identified with the classical result for radiative energy transfer.

Examining the time-ordered diagram of Fig. 4(a), and considering the case where the two centers are far enough apart that the photon mediating the energy transfer between them can be considered as real and observable, the processes occurring at A_1 and A_2 can be regarded as distinct, Fig. 4(b). Hence, in the long-range limit, the two-beam cooperative two-photon absorption process under consideration here is analogous to a two-beam hyper-Raman process at one center, followed by single-photon absorption at the other. The purpose of this section is to conduct a detailed examination of this analogy, and, ultimately, to demonstrate an exact correspondence between the two descriptions.

A. Hyper-Raman scattering at A_1

A two-beam hyper-Raman process at the center A_1 results in emission of a photon with frequency $\omega' = ck'$ and polarization \mathbf{e}' , where energy conservation dictates that

$$\hbar ck' = \hbar \omega_1 + \hbar \omega_2 - E_{\alpha 0}. \quad (3.1)$$

The corresponding rate associated with the emission of $(\mathbf{k}', \mathbf{e}')$ is calculated using the standard methods of molecular quantum electrodynamics, utilizing the time-ordered diagram on the left-hand side of Fig. 4(b). This leads to an expression for the matrix element;

$$M_{fi} = (\hbar c / 2V\epsilon_0)^{3/2} (n_1 n_2 k_1 k_2 k')^{1/2} \bar{e}'_{3i} e_{2j} e_{1k} \bar{e}_{2m} \bar{e}_{1n} \beta_{ijk}^{\alpha 0}, \quad (3.2)$$

where $\beta_{ijk}^{\alpha 0}$ is the two-beam hyper-Raman β tensor,¹⁴ and all the other symbols have their usual meaning. The rate of emission into an element of solid angle $d\Omega$ is then given by

$$\Gamma = \frac{\hbar c^2}{32\pi^2 V^2 \epsilon_0^3} n_1 n_2 k_1 k_2 k'^3 \bar{e}'_{3i} e_{2j} e_{1k} \bar{e}_{2m} \bar{e}_{1n} \beta_{ijk}^{\alpha 0} \bar{\beta}_{lmn}^{\alpha 0} d\Omega, \quad (3.3)$$

in which use has been made of the Fermi golden rule, and the result

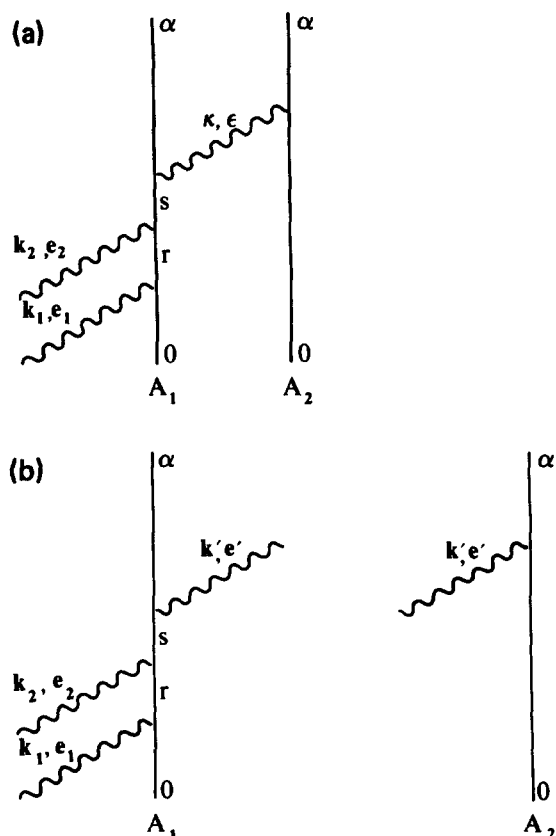


FIG. 4. Time-ordered diagrams illustrating (a) a typical distributive two-frequency two-photon absorption process, and (b) two beam hyper-Raman at A_1 with single-frequency absorption at A_2 .

$$\rho_f = \frac{k'^2 V}{8\pi^3 \hbar c} d\Omega, \quad (3.4)$$

for the density of final states. The radiant intensity of emission, defined as the power per unit solid angle around k' , can

be obtained by multiplying the rate of emission by the scattered photon energy, i.e.,

$$I(k') = \Gamma \times \hbar c k' \quad (3.5)$$

$$= \frac{\hbar^2 c^3}{32\pi^2 V^2 \epsilon_0^3} n_1 n_2 k_1 k_2 k'^4 \bar{e}_{3i} e_{2j} e_{1k} e'_{3l} \bar{e}_{2m} \times \bar{e}_{1n} \beta_{ijk}^{\alpha 0} \bar{\beta}_{lmn}^{\alpha 0} d\Omega. \quad (3.6)$$

To obtain a completely general irradiance for double-beam hyper-Raman emission from a collection of randomly oriented molecules requires further development of Eq. (3.6). Direct averaging entails performing a sum over virtual photon polarizations, together with a lengthy sixth-rank average. However, it is possible to arrive at a general, fully averaged, rate through a different, though completely equivalent, series of procedures.¹⁸

Initially a summation is performed over the polarizations of the emitted photon, for a given emission direction. This is achieved by means of the formula¹⁹

$$\sum_{\lambda} \bar{e}_{3i}^{(\lambda)} e_{3l}^{(\lambda)} = \delta_{il} - \hat{k}_{3i} \hat{k}_{3l}. \quad (3.7)$$

The hyper-Raman intensity is then spherically averaged over all directions of emission, using the fact that

$$\langle (\delta_{il} - \hat{k}_{3i} \hat{k}_{3l}) \beta_{ijk}^{\alpha 0} \bar{\beta}_{lmn}^{\alpha 0} \rangle = \frac{1}{3} \beta_{ijk}^{\alpha 0} \bar{\beta}_{lmn}^{\alpha 0}. \quad (3.8)$$

Hence, the integrated hyper-Raman intensity, or radiant power, is given by

$$\begin{aligned} \phi &= \int_{4\pi} I(k') d\Omega \\ &= \frac{\hbar^2 c^3}{12\pi V^2 \epsilon_0^3} n_1 n_2 k_1 k_2 k'^4 e_{2j} e_{1k} \bar{e}_{2m} \bar{e}_{1n} \beta_{ijk}^{\alpha 0} \bar{\beta}_{lmn}^{\alpha 0} d\Omega. \end{aligned} \quad (3.9) \quad (3.10)$$

The result, Eq. (3.10), must then be further averaged to account for the random assembly of molecules. The calculation then requires a standard fourth-rank average, and yields

$$\phi = \frac{I_1 I_2 k'^4}{360\pi c \epsilon_0^3} \begin{bmatrix} |e_1 \cdot e_2|^2 \\ 1 \\ |e_1 \cdot \bar{e}_2|^2 \end{bmatrix}^T \begin{bmatrix} 4 & -1 & -1 \\ -1 & 4 & -1 \\ -1 & -1 & 4 \end{bmatrix} \begin{bmatrix} \beta_{\lambda\mu\mu}^{\alpha 0} \bar{\beta}_{\lambda\nu\nu}^{\alpha 0} \\ \beta_{\lambda\mu\nu}^{\alpha 0} \bar{\beta}_{\lambda\mu\nu}^{\alpha 0} \\ \beta_{\lambda\mu\nu}^{\alpha 0} \bar{\beta}_{\lambda\nu\mu}^{\alpha 0} \end{bmatrix}. \quad (3.11)$$

Equation (3.11) represents the total radiant power for the hyper-Raman process. To obtain the irradiance at a distance R from the emitting molecule requires division by the surface area of a sphere of radius R . Consequently, the irradiance $I(k')$, resulting from hyper-Raman scattering, at a distance R from the emitting molecule is

$$I(k') = \frac{\phi}{4\pi R^2} = \frac{I_1 I_2 k'^4}{1440\pi^2 c \epsilon_0^3 R^2} \begin{bmatrix} |e_1 \cdot e_2|^2 \\ 1 \\ |e_1 \cdot \bar{e}_2|^2 \end{bmatrix}^T \begin{bmatrix} 4 & -1 & -1 \\ -1 & 4 & -1 \\ -1 & -1 & 4 \end{bmatrix} \begin{bmatrix} \beta_{\lambda\mu\mu}^{\alpha 0} \bar{\beta}_{\lambda\nu\nu}^{\alpha 0} \\ \beta_{\lambda\mu\nu}^{\alpha 0} \bar{\beta}_{\lambda\mu\nu}^{\alpha 0} \\ \beta_{\lambda\mu\nu}^{\alpha 0} \bar{\beta}_{\lambda\nu\mu}^{\alpha 0} \end{bmatrix}. \quad (3.12)$$

B. Absorption of the hyper-Raman radiation at A_2

The process of single-photon absorption is, mathematically, quite simple. The matrix element is immediately derived from the time-ordered diagram on the right-hand side of Fig. 4(b), and its evaluation leads to an averaged rate given by

$$\langle \Gamma \rangle = \frac{\pi \rho_f I}{3\hbar c \epsilon_0} |\mu^{\alpha 0}|^2, \quad (3.13)$$

where I is the irradiance of the incident beam. Now, to calculate the overall rate of hyper-Raman at A_1 followed by absorption at the emitted photon at A_2 requires substitution of the equation for the irradiance of $(\mathbf{k}', \mathbf{e}')$ photons, Eq. (3.12), into Eq. (3.13) producing

$$\langle \Gamma \rangle = \frac{I_1 I_2 k'^4 \rho_f}{4320 \pi \hbar c^2 \epsilon_0^4 R^2} \begin{bmatrix} |\mathbf{e}_1 \cdot \mathbf{e}_2|^2 \\ 1 \\ |\mathbf{e}_1 \cdot \bar{\mathbf{e}}_2|^2 \end{bmatrix}^T \begin{bmatrix} 4 & -1 & -1 \\ -1 & 4 & -1 \\ -1 & -1 & 4 \end{bmatrix} \begin{bmatrix} \beta_{\lambda\mu\mu}^{\alpha 0} \bar{\beta}_{\lambda\nu\nu}^{\alpha 0} \\ \beta_{\lambda\mu\nu}^{\alpha 0} \bar{\beta}_{\lambda\mu\nu}^{\alpha 0} \\ \beta_{\lambda\mu\nu}^{\alpha 0} \bar{\beta}_{\lambda\nu\mu}^{\alpha 0} \end{bmatrix} |\mu^{\alpha 0}|^2. \quad (3.14)$$

C. The long-range limit of two-beam mean-frequency absorption

To complete the comparison between the long-range limit of two-beam mean-frequency absorption, and hyper-Raman scattering followed by absorption of the scattered radiation, it is necessary to reexamine the time-ordered diagrams of Fig. 3, and the corresponding matrix element. Clearly, since the case under consideration involves hyper-Raman at A_1 and absorption at A_2 , it would be incorrect to include contributions from time-ordered diagrams of the type shown in Figs. 3(c) and 3(d). Only those of the type shown in Figs. 3(a) and 3(b) contribute, and hence consideration need only be given to the first term in the curly brackets of Eq. (2.1). This leads to the following rate equation;

$$\langle \Gamma \rangle = \frac{\hbar c^2 \pi \rho_f n_1 n_2 k_1 k_2}{60 V^2 \epsilon_0^2} \begin{bmatrix} |\mathbf{e}_1 \cdot \mathbf{e}_2|^2 \\ 1 \\ |\mathbf{e}_1 \cdot \bar{\mathbf{e}}_2|^2 \end{bmatrix}^T \begin{bmatrix} 4 & -1 & -1 \\ -1 & 4 & -1 \\ -1 & -1 & 4 \end{bmatrix} \begin{bmatrix} \beta_{kii}^{\alpha 0} \bar{\beta}_{njj}^{\alpha 0} \\ \beta_{kij}^{\alpha 0} \bar{\beta}_{njj}^{\alpha 0} \\ \beta_{kij}^{\alpha 0} \bar{\beta}_{nji}^{\alpha 0} \end{bmatrix} \mu_{li} \bar{\mu}_p V_{kl}(\gamma, \mathbf{R}) \bar{V}_{np}(\gamma, \mathbf{R}), \quad (3.15)$$

where a fourth-rank average has been performed to account for the random orientation of the A_1 - A_2 molecular pair with respect to the laser beam polarizations. To facilitate comparison with the result obtained in Sec. III B, the above equation has been recast in terms of the tensor $\beta_{ijk}^{\alpha 0} \equiv \chi_{jki}^{\alpha 0}$. Further averaging is now required to account for the random orientation of the intermolecular displacement vector, and also the random orientation of the two centers with respect to one another.

$$\langle \Gamma \rangle = \frac{\hbar c^2 \pi \rho_f n_1 n_2 k_1 k_2}{540 V^2 \epsilon_0^2} \begin{bmatrix} |\mathbf{e}_1 \cdot \mathbf{e}_2|^2 \\ 1 \\ |\mathbf{e}_1 \cdot \bar{\mathbf{e}}_2|^2 \end{bmatrix}^T \begin{bmatrix} 4 & -1 & -1 \\ -1 & 4 & -1 \\ -1 & -1 & 4 \end{bmatrix} \begin{bmatrix} \beta_{kii}^{\alpha 0} \bar{\beta}_{kjj}^{\alpha 0} \\ \beta_{kij}^{\alpha 0} \bar{\beta}_{kij}^{\alpha 0} \\ \beta_{kij}^{\alpha 0} \bar{\beta}_{kji}^{\alpha 0} \end{bmatrix} |\mu^{\alpha 0}|^2 V_{lm}(\gamma, \mathbf{R}) \bar{V}_{lm}(\gamma, \mathbf{R}). \quad (3.16)$$

Rewriting Eq. (3.16) in terms of the irradiances of the incident beams gives

$$\langle \Gamma \rangle = \frac{I_1 I_2 \pi \rho_f}{540 \hbar c^2 \epsilon_0^2} \begin{bmatrix} |\mathbf{e}_1 \cdot \mathbf{e}_2|^2 \\ 1 \\ |\mathbf{e}_1 \cdot \bar{\mathbf{e}}_2|^2 \end{bmatrix}^T \begin{bmatrix} 4 & -1 & -1 \\ -1 & 4 & -1 \\ -1 & -1 & 4 \end{bmatrix} \begin{bmatrix} \beta_{kii}^{\alpha 0} \bar{\beta}_{kjj}^{\alpha 0} \\ \beta_{kij}^{\alpha 0} \bar{\beta}_{kij}^{\alpha 0} \\ \beta_{kij}^{\alpha 0} \bar{\beta}_{kji}^{\alpha 0} \end{bmatrix} |\mu^{\alpha 0}|^2 V_{lm}(\gamma, \mathbf{R}) \bar{V}_{lm}(\gamma, \mathbf{R}). \quad (3.17)$$

The full expression for the retarded resonance electric dipole-electric dipole interaction is given in Eq. (2.2), and the long-range limit of $V_{lm}(\gamma, \mathbf{R}) \bar{V}_{lm}(\gamma, \mathbf{R})$ is easily shown to be

$$\lim_{\gamma R \gg 1} V_{lm}(\gamma, \mathbf{R}) \bar{V}_{lm}(\gamma, \mathbf{R}) = \frac{\gamma^4}{8 \pi^2 R^2 \epsilon_0^2}. \quad (3.18)$$

Hence, the long-range limit of the fully averaged result is

$$\langle \Gamma \rangle = \frac{I_1 I_2 \gamma^4 \rho_f}{4320 \pi \hbar c^2 \epsilon_0^4 R^2} \begin{bmatrix} |\mathbf{e}_1 \cdot \mathbf{e}_2|^2 \\ 1 \\ |\mathbf{e}_1 \cdot \bar{\mathbf{e}}_2|^2 \end{bmatrix}^T \begin{bmatrix} 4 & -1 & -1 \\ -1 & 4 & -1 \\ -1 & -1 & 4 \end{bmatrix} \begin{bmatrix} \beta_{\lambda\mu\mu}^{\alpha 0} \bar{\beta}_{\lambda\nu\nu}^{\alpha 0} \\ \beta_{\lambda\mu\nu}^{\alpha 0} \bar{\beta}_{\lambda\mu\nu}^{\alpha 0} \\ \beta_{\lambda\mu\nu}^{\alpha 0} \bar{\beta}_{\lambda\nu\mu}^{\alpha 0} \end{bmatrix} |\mu^{\alpha 0}|^2. \quad (3.19)$$

Since γ effectively represents the conservation energy transferred between the two centers by the virtual photon, in the long-range limit where the photon is considered to be physically identifiable γ can be directly equated with k' , (the wave vector of the hyper-Raman photon). Hence, Eq. (3.19) becomes exactly equivalent to Eq. (3.14), i.e., the long-range limit of distributive two-beam two-photon absorption is equivalent to a process of hyper-Raman at one center followed by single-photon absorption of the hyper-Raman emission at the second center.

IV. DISCUSSION

Although this paper is the fourth of a series under the general theme of concerted two-photon absorption, a distinction has now been drawn between the two alternative mechanisms by which the process may take place. The term *cooperative* has now been reserved for the mechanism where one real photon is absorbed at each of the two centers involved in the process, and the term *distributive* for the case where both real photons are absorbed at one of the centers.

This paper deals specifically with the theory of distributive two-beam two-photon absorption, but many of the remarks which were made in earlier work⁷ apply equally here. The selection rules for distributive absorption are essentially those of single-photon absorption, since although one center experiences *three* photon interactions (two real and one virtual) any transition which is one-photon allowed is also three-photon allowed. Although the converse is not universally true, three-photon allowed transitions which are *not* one-photon allowed (in the electric-dipole approximation) only arise in molecules of very high symmetry.¹³ Clearly in molecules possessing a center of inversion selection rules dictate that the distributive and cooperative mechanisms for excitation to any particular energy level are mutually exclusive.

It is interesting to note that although one of the two absorbing centers must be irradiated by both beams, the second center absorbs only a virtual photon and need not, therefore, be within the volume of sample irradiated by either beam. This has an unusual consequence for the case where the two centers are discrete molecules. The number of potential partners A_2 which may be involved in the distributive excitation of any particular molecule A_1 greatly exceeds the number available for cooperative excitation, and, assuming a uniform sample density, increases with the square of the intermolecular distance. Since the long-range form of the rate equation has an *inverse-square* dependence on the separation, this implies that the sum of all contributions from partner molecules within a shell of given thickness centered on A_1 is, in the long-range limit, independent of the shell radius. This surprising result is a molecular analog of the astrophysical problem known as Olber's Paradox, which raises the question as to why the sky is not uniformly bright with starlight. This paradox arises in a similar way since, although starlight intensity drops off with the square of distance, the number of stars in a homogeneous universe also increases quadratically with distance from any given point. In both cases the resolution of the paradox is connected with a consideration of the neglected effects of light scattering.

While inverse-square rate-dependences of this type are rare and therefore often suspect in *atomic and molecular* physics, the comparison between the results for distributive mean-frequency absorption based on virtual photon coupling, and hyper-Raman scattering followed by absorption, has shown the two processes to be *precisely* equivalent in the long-range limit. Since the latter has the R^{-2} dependence associated with any macroscopic radiative process, the comparison establishes the correctness of the long-range distance dependence of the virtual photon coupling. Despite this concentration on long-range behavior, it must nonetheless be stressed that the effect described is *predominantly* effective over very short distances, and is a proximity-induced interaction.²⁰

ACKNOWLEDGMENT

K.P.H. gratefully acknowledges financial support from the S.E.R.C.

APPENDIX

Explicit form of the molecular tensor invariants,
 $T^{(j,q)}(A_1, A_2, A_2, A_1) = Z_{\rho\sigma\tau}^{(j,q)}(A_1, A_2, A_2, A_1) V_{\rho\rho}(\gamma, \mathbf{R}) \bar{V}_{\sigma\tau}(\gamma, \mathbf{R})$:

j	q	$Z_{\rho\sigma\tau}^{(j,q)}(A_1, A_2, A_2, A_1)$
0	1	$\chi_{\lambda\lambda\pi}^{\alpha\alpha}(A_1) \mu_{\rho}^{\alpha\alpha}(A_2) \bar{\chi}_{\mu\mu\sigma}^{\alpha\alpha}(A_2) \bar{\mu}_{\tau}^{\alpha\alpha}(A_1)$
0	2	$\chi_{\lambda\mu\pi}^{\alpha\alpha}(A_1) \mu_{\rho}^{\alpha\alpha}(A_2) \bar{\chi}_{\lambda\mu\sigma}^{\alpha\alpha}(A_2) \bar{\mu}_{\tau}^{\alpha\alpha}(A_1)$
0	3	$\chi_{\lambda\mu\pi}^{\alpha\alpha}(A_1) \mu_{\rho}^{\alpha\alpha}(A_2) \bar{\chi}_{\mu\lambda\sigma}^{\alpha\alpha}(A_2) \bar{\mu}_{\tau}^{\alpha\alpha}(A_1)$
1	1	$\epsilon_{\lambda\mu\nu} \hat{R}_{\nu} \chi_{\lambda\mu\pi}^{\alpha\alpha}(A_1) \mu_{\rho}^{\alpha\alpha}(A_2) \bar{\chi}_{\mu\sigma\sigma}^{\alpha\alpha}(A_2) \bar{\mu}_{\tau}^{\alpha\alpha}(A_1)$
1	2	$\epsilon_{\lambda\mu\nu} \hat{R}_{\nu} \chi_{\lambda\mu\pi}^{\alpha\alpha}(A_1) \mu_{\rho}^{\alpha\alpha}(A_2) \bar{\chi}_{\mu\sigma\sigma}^{\alpha\alpha}(A_2) \bar{\mu}_{\tau}^{\alpha\alpha}(A_1)$
1	3	$\epsilon_{\lambda\mu\nu} \hat{R}_{\nu} \chi_{\lambda\mu\pi}^{\alpha\alpha}(A_1) \mu_{\rho}^{\alpha\alpha}(A_2) \bar{\chi}_{\mu\sigma\sigma}^{\alpha\alpha}(A_2) \bar{\mu}_{\tau}^{\alpha\alpha}(A_1)$
1	4	$\epsilon_{\mu\sigma\nu} \hat{R}_{\nu} \chi_{\lambda\mu\pi}^{\alpha\alpha}(A_1) \mu_{\rho}^{\alpha\alpha}(A_2) \bar{\chi}_{\mu\sigma\sigma}^{\alpha\alpha}(A_2) \bar{\mu}_{\tau}^{\alpha\alpha}(A_1)$
1	5	$\epsilon_{\mu\sigma\nu} \hat{R}_{\nu} \chi_{\lambda\mu\pi}^{\alpha\alpha}(A_1) \mu_{\rho}^{\alpha\alpha}(A_2) \bar{\chi}_{\mu\sigma\sigma}^{\alpha\alpha}(A_2) \bar{\mu}_{\tau}^{\alpha\alpha}(A_1)$
1	6	$\epsilon_{\mu\sigma\nu} \hat{R}_{\nu} \chi_{\lambda\lambda\pi}^{\alpha\alpha}(A_1) \mu_{\rho}^{\alpha\alpha}(A_2) \bar{\chi}_{\mu\sigma\sigma}^{\alpha\alpha}(A_2) \bar{\mu}_{\tau}^{\alpha\alpha}(A_1)$
2	1	$\hat{R}_{\mu} \hat{R}_{\nu} \chi_{\lambda\lambda\pi}^{\alpha\alpha}(A_1) \mu_{\rho}^{\alpha\alpha}(A_2) \bar{\chi}_{\mu\nu\sigma}^{\alpha\alpha}(A_2) \bar{\mu}_{\tau}^{\alpha\alpha}(A_1)$ $- \frac{1}{3} \chi_{\lambda\lambda\pi}^{\alpha\alpha}(A_1) \mu_{\rho}^{\alpha\alpha}(A_2) \bar{\chi}_{\mu\mu\sigma}^{\alpha\alpha}(A_2) \bar{\mu}_{\tau}^{\alpha\alpha}(A_1)$
2	2	$\hat{R}_{\mu} \hat{R}_{\nu} \chi_{\lambda\mu\pi}^{\alpha\alpha}(A_1) \mu_{\rho}^{\alpha\alpha}(A_2) \bar{\chi}_{\lambda\nu\sigma}^{\alpha\alpha}(A_2) \bar{\mu}_{\tau}^{\alpha\alpha}(A_1)$ $- \frac{1}{3} \chi_{\lambda\mu\pi}^{\alpha\alpha}(A_1) \mu_{\rho}^{\alpha\alpha}(A_2) \bar{\chi}_{\lambda\mu\sigma}^{\alpha\alpha}(A_2) \bar{\mu}_{\tau}^{\alpha\alpha}(A_1)$
2	3	$\hat{R}_{\mu} \hat{R}_{\nu} \chi_{\lambda\mu\pi}^{\alpha\alpha}(A_1) \mu_{\rho}^{\alpha\alpha}(A_2) \bar{\chi}_{\lambda\nu\sigma}^{\alpha\alpha}(A_2) \bar{\mu}_{\tau}^{\alpha\alpha}(A_1)$ $- \frac{1}{3} \chi_{\lambda\mu\pi}^{\alpha\alpha}(A_1) \mu_{\rho}^{\alpha\alpha}(A_2) \bar{\chi}_{\mu\lambda\sigma}^{\alpha\alpha}(A_2) \bar{\mu}_{\tau}^{\alpha\alpha}(A_1)$
2	4	$\hat{R}_{\lambda} \hat{R}_{\nu} \chi_{\lambda\mu\pi}^{\alpha\alpha}(A_1) \mu_{\rho}^{\alpha\alpha}(A_2) \bar{\chi}_{\mu\nu\sigma}^{\alpha\alpha}(A_2) \bar{\mu}_{\tau}^{\alpha\alpha}(A_1)$ $- \frac{1}{3} \chi_{\lambda\mu\pi}^{\alpha\alpha}(A_1) \mu_{\rho}^{\alpha\alpha}(A_2) \bar{\chi}_{\mu\lambda\sigma}^{\alpha\alpha}(A_2) \bar{\mu}_{\tau}^{\alpha\alpha}(A_1)$
2	5	$\hat{R}_{\lambda} \hat{R}_{\nu} \chi_{\lambda\mu\pi}^{\alpha\alpha}(A_1) \mu_{\rho}^{\alpha\alpha}(A_2) \bar{\chi}_{\mu\nu\sigma}^{\alpha\alpha}(A_2) \bar{\mu}_{\tau}^{\alpha\alpha}(A_1)$ $- \frac{1}{3} \chi_{\lambda\mu\pi}^{\alpha\alpha}(A_1) \mu_{\rho}^{\alpha\alpha}(A_2) \bar{\chi}_{\lambda\mu\sigma}^{\alpha\alpha}(A_2) \bar{\mu}_{\tau}^{\alpha\alpha}(A_1)$
2	6	$\hat{R}_{\lambda} \hat{R}_{\mu} \chi_{\lambda\mu\pi}^{\alpha\alpha}(A_1) \mu_{\rho}^{\alpha\alpha}(A_2) \bar{\chi}_{\nu\sigma\sigma}^{\alpha\alpha}(A_2) \bar{\mu}_{\tau}^{\alpha\alpha}(A_1)$ $- \frac{1}{3} \chi_{\lambda\lambda\pi}^{\alpha\alpha}(A_1) \mu_{\rho}^{\alpha\alpha}(A_2) \bar{\chi}_{\mu\mu\sigma}^{\alpha\alpha}(A_2) \bar{\mu}_{\tau}^{\alpha\alpha}(A_1)$
3	1	$1/5 \epsilon_{\lambda\mu\nu} \{ 5 \hat{R}_{\nu} \hat{R}_{\xi} \hat{R}_{\sigma} \chi_{\lambda\xi\pi}^{\alpha\alpha}(A_1) \mu_{\rho}^{\alpha\alpha}(A_2)$ $\times \bar{\chi}_{\mu\sigma\sigma}^{\alpha\alpha}(A_2) \bar{\mu}_{\tau}^{\alpha\alpha}(A_1)$ $- \hat{R}_{\sigma} \chi_{\lambda\nu\pi}^{\alpha\alpha}(A_1) \mu_{\rho}^{\alpha\alpha}(A_2) \bar{\chi}_{\mu\sigma\sigma}^{\alpha\alpha}(A_2) \bar{\mu}_{\tau}^{\alpha\alpha}(A_1)$ $- \hat{R}_{\sigma} \chi_{\lambda\sigma\pi}^{\alpha\alpha}(A_1) \mu_{\rho}^{\alpha\alpha}(A_2) \bar{\chi}_{\mu\nu\sigma}^{\alpha\alpha}(A_2) \bar{\mu}_{\tau}^{\alpha\alpha}(A_1)$ $- \hat{R}_{\nu} \chi_{\lambda\sigma\pi}^{\alpha\alpha}(A_1) \mu_{\rho}^{\alpha\alpha}(A_2) \bar{\chi}_{\mu\sigma\sigma}^{\alpha\alpha}(A_2) \bar{\mu}_{\tau}^{\alpha\alpha}(A_1) \}$
3	2	$1/5 \epsilon_{\lambda\mu\nu} \{ 5 \hat{R}_{\nu} \hat{R}_{\xi} \hat{R}_{\sigma} \chi_{\xi\lambda\pi}^{\alpha\alpha}(A_1) \mu_{\rho}^{\alpha\alpha}(A_2)$ $\times \bar{\chi}_{\mu\sigma\sigma}^{\alpha\alpha}(A_2) \bar{\mu}_{\tau}^{\alpha\alpha}(A_1)$ $- \hat{R}_{\sigma} \chi_{\nu\lambda\pi}^{\alpha\alpha}(A_1) \mu_{\rho}^{\alpha\alpha}(A_2) \bar{\chi}_{\mu\sigma\sigma}^{\alpha\alpha}(A_2) \bar{\mu}_{\tau}^{\alpha\alpha}(A_1)$ $- \hat{R}_{\sigma} \chi_{\sigma\lambda\pi}^{\alpha\alpha}(A_1) \mu_{\rho}^{\alpha\alpha}(A_2) \bar{\chi}_{\mu\nu\sigma}^{\alpha\alpha}(A_2) \bar{\mu}_{\tau}^{\alpha\alpha}(A_1)$ $- \hat{R}_{\nu} \chi_{\sigma\lambda\pi}^{\alpha\alpha}(A_1) \mu_{\rho}^{\alpha\alpha}(A_2) \bar{\chi}_{\mu\sigma\sigma}^{\alpha\alpha}(A_2) \bar{\mu}_{\tau}^{\alpha\alpha}(A_1) \}$
3	3	$1/5 \epsilon_{\lambda\mu\nu} \{ 5 \hat{R}_{\nu} \hat{R}_{\xi} \hat{R}_{\sigma} \chi_{\xi\sigma\pi}^{\alpha\alpha}(A_1) \mu_{\rho}^{\alpha\alpha}(A_2)$ $\times \bar{\chi}_{\lambda\mu\sigma}^{\alpha\alpha}(A_2) \bar{\mu}_{\tau}^{\alpha\alpha}(A_1)$ $- \hat{R}_{\sigma} \chi_{\nu\sigma\pi}^{\alpha\alpha}(A_1) \mu_{\rho}^{\alpha\alpha}(A_2) \bar{\chi}_{\lambda\mu\sigma}^{\alpha\alpha}(A_2) \bar{\mu}_{\tau}^{\alpha\alpha}(A_1)$ $- \hat{R}_{\sigma} \chi_{\sigma\nu\pi}^{\alpha\alpha}(A_1) \mu_{\rho}^{\alpha\alpha}(A_2) \bar{\chi}_{\lambda\mu\sigma}^{\alpha\alpha}(A_2) \bar{\mu}_{\tau}^{\alpha\alpha}(A_1)$ $- \hat{R}_{\nu} \chi_{\sigma\sigma\pi}^{\alpha\alpha}(A_1) \mu_{\rho}^{\alpha\alpha}(A_2) \bar{\chi}_{\lambda\mu\sigma}^{\alpha\alpha}(A_2) \bar{\mu}_{\tau}^{\alpha\alpha}(A_1) \}$
4	1	$\hat{R}_{\lambda} \hat{R}_{\mu} \hat{R}_{\nu} \hat{R}_{\sigma} \chi_{\lambda\mu\pi}^{\alpha\alpha}(A_1) \mu_{\rho}^{\alpha\alpha}(A_2) \bar{\chi}_{\nu\sigma\sigma}^{\alpha\alpha}(A_2) \bar{\mu}_{\tau}^{\alpha\alpha}(A_1)$ $- 1/7 \{ \chi_{\lambda\lambda\pi}^{\alpha\alpha}(A_1) \mu_{\rho}^{\alpha\alpha}(A_2)$ $\times \bar{\chi}_{\nu\sigma\sigma}^{\alpha\alpha}(A_2) \bar{\mu}_{\tau}^{\alpha\alpha}(A_1) \hat{R}_{\nu} \hat{R}_{\sigma}$ $+ \chi_{\lambda\nu\pi}^{\alpha\alpha}(A_1) \mu_{\rho}^{\alpha\alpha}(A_2) \bar{\chi}_{\lambda\sigma\sigma}^{\alpha\alpha}(A_2) \bar{\mu}_{\tau}^{\alpha\alpha}(A_1) \hat{R}_{\nu} \hat{R}_{\sigma}$ $+ \chi_{\lambda\nu\pi}^{\alpha\alpha}(A_1) \mu_{\rho}^{\alpha\alpha}(A_2) \bar{\chi}_{\sigma\lambda\sigma}^{\alpha\alpha}(A_2) \bar{\mu}_{\tau}^{\alpha\alpha}(A_1) \hat{R}_{\nu} \hat{R}_{\sigma}$ $+ \chi_{\nu\lambda\pi}^{\alpha\alpha}(A_1) \mu_{\rho}^{\alpha\alpha}(A_2) \bar{\chi}_{\lambda\sigma\sigma}^{\alpha\alpha}(A_2) \bar{\mu}_{\tau}^{\alpha\alpha}(A_1) \hat{R}_{\nu} \hat{R}_{\sigma}$

$$\begin{aligned}
& + \chi_{\nu\mu\pi}^{\alpha 0}(A_1)\mu_{\rho}^{\alpha 0}(A_2)\bar{\chi}_{\alpha\mu\sigma}^{\alpha 0}(A_2)\bar{\mu}_{\tau}^{\alpha 0}(A_1)\hat{R}_{\nu}\hat{R}_{\sigma} \\
& + \chi_{\nu\sigma\pi}^{\alpha 0}(A_1)\mu_{\rho}^{\alpha 0}(A_2)\bar{\chi}_{\lambda\lambda\sigma}^{\alpha 0}(A_2)\bar{\mu}_{\tau}^{\alpha 0}(A_1)\hat{R}_{\nu}\hat{R}_{\sigma} \} \\
& + 1/35\{\chi_{\lambda\lambda\pi}^{\alpha 0}(A_1)\mu_{\rho}^{\alpha 0}(A_2) \\
& \times \bar{\chi}_{\mu\mu\sigma}^{\alpha 0}(A_2)\bar{\mu}_{\tau}^{\alpha 0}(A_1) \\
& + \chi_{\lambda\mu\pi}^{\alpha 0}(A_1)\mu_{\rho}^{\alpha 0}(A_2)\bar{\chi}_{\lambda\mu\sigma}^{\alpha 0}(A_2)\bar{\mu}_{\tau}^{\alpha 0}(A_1) \\
& + \chi_{\lambda\mu\pi}^{\alpha 0}(A_1)\mu_{\rho}^{\alpha 0}(A_2)\bar{\chi}_{\mu\lambda\sigma}^{\alpha 0}(A_2)\bar{\mu}_{\tau}^{\alpha 0}(A_1)\}
\end{aligned}$$

¹S. Geltman, Phys. Rev. A **35**, 3775 (1987).

²I. Last, Y. S. Kim and T. F. George, Chem. Phys. Lett. **138**, 225 (1987).

³M. E. Fajardo and V. A. Apkarian, Chem. Phys. Lett. **134**, 55 (1987).

⁴M. E. Fajardo and V. A. Apkarian, J. Chem. Phys. **85**, 5660 (1986).

⁵D. L. Andrews and M. J. Harlow, J. Chem. Phys. **78**, 1088 (1983).

⁶D. L. Andrews and M. J. Harlow, J. Chem. Phys. **80**, 4753 (1984).

⁷D. L. Andrews and K. P. Hopkins, J. Chem. Phys. **86**, 2453 (1987).

⁸R. J. Locke and E. C. Lim, Chem. Phys. Lett. **134**, 107 (1987).

⁹E. A. Power, *Introductory Quantum Electrodynamics* (Longmans, New York, 1964).

¹⁰D. P. Craig and T. Thirunamachandran, *Molecular Quantum Electrodynamics* (Academic, London, 1984).

¹¹E. A. Power and T. Thirunamachandran, Phys. Rev. A **28**, 2671 (1983).

¹²D. L. Andrews and B. S. Sherborne, J. Chem. Phys. **86**, 4011 (1987).

¹³D. L. Andrews and P. J. Wilkes, J. Chem. Phys. **83**, 2009 (1985).

¹⁴D. L. Andrews and T. Thirunamachandran, J. Chem. Phys. **68**, 2941 (1978).

¹⁵D. L. Andrews and M. J. Harlow, Phys. Rev. A **29**, 2796 (1984).

¹⁶D. L. Andrews and T. Thirunamachandran, J. Chem. Phys. **67**, 5026 (1977).

¹⁷D. L. Andrews and W. A. Ghoul, Phys. Rev. A **25**, 2647 (1982). Refer to the right-hand column of Table I, where the heading should read $g_{(A,J)}^{\alpha}$ rather than g^{α} .

¹⁸D. L. Andrews, Mol. Phys. **52**, 969 (1984).

¹⁹W. P. Healy, *Non-relativistic Quantum Electrodynamics* (Academic, London, 1982).

²⁰D. L. Andrews and K. P. Hopkins, J. Mol. Struct. **175**, 141 (1988).